Behavior of Radionuclides during Acidic Leaching Processes of Different Rock Materials, Allouga Locality, Southwestern Sinai, Egypt

Ibrahim E. El Aassy, Mohamed G. El Feky, Mohamed. A. El Kasaby, Eman M. Ibrahim, Salwa Sewefi, Reda M. Attia

Abstract

To study radionuclides transfer from solid material (ore) to the liquid phase (leachate), ten samples of different rock types were collected and prepared for various analyses. Wet chemical analyses were carried out for major oxides and trace elements. Natural radionuclides contents were measured by γ-ray spectrometry employing a high purity germanium (HPGe) detector in original samples, pregnant solutions, and residuals. The variables in this study are different rock types and different radionuclides. These variables played a role in the transfer of different radionuclides from solid (original sample) to solution (leachate), and from solution to back to solid (residual). The results show that the transfer of radionuclides was carried out either physically through α-recoil or chemically through dissolution, complexation, chelation, and ion-adsorption. The rock type played a role in migration of radionuclides, especially thorium isotopes (^{234}Th, ^{232}Th, and ^{230}Th). The high organic matter samples showed relatively high migration for these isotopes. High-carbonate samples showed very low leachability for ^{238}U and ^{235}U; ^{234}U was higher at 28.84%, but this value also is low when compared to corresponding values in samples of other rock types. The low leachability in carbonate rocks may be due to the high consumption of acid due to high carbonate content.

Keywords: Radionuclides; Leaching; α-recoil; Sinai

1 Introduction

Uranium is a naturally occurring radionuclide which has three isotopes: ^{238}U, ^{235}U, and ^{234}U. The radiological half-lives of these isotopes are 4.5 x 10^9, 7.1 x 10^8, and 2.5 x 10^5 years, respectively. ^{238}U and ^{235}U are parent radionuclides of two naturally occurring radioactive series. The mass percentages of ^{238}U, ^{235}U, and ^{234}U in natural uranium are 99.27, 0.72, and 0.005%, respectively. Two stems in the ^{238}U decay series are ^{230}Th (7.5 x 10^4 years) and ^{226}Ra (1600 years). These and ^{234}U are suitable for use as geochemical tracers and can be of enormous value in researching the behavior of radionuclides through leaching of various radioactive rock types.

The basic rule of U-disequilibrium study is that after a period of time of about 5-6 half-lives of daughter, the parent and the daughter will have similar activities and if there is no disturbance in the system, then the ratio of activities are equal to unity, a state termed secular equilibrium. If there is a disturbance by any process resulting in a net removal or addition of either of the two, the activity ratio is no longer unity but departs from the equilibrium value to an extent that depends on the characteristics of the disturbance. This is the state of disequilibrium.

- *Ibrahim E. El Aassy, Prof. of Nuclear Ores, Nuclear Materials Authority, Cairo, Egypt. E-mail: elaassy_2011@yahoo.com*
- *Mohamed G. El Feky, Prof. of Geochemistry, Nuclear Materials Authority, Cairo, Egypt. E-mail: mohamed.galal391@yahoo.com*
- *Mohamed A. El Kasaby, Prof. of Organic Chemistry Ain Shams University, Cairo, Egypt.*
- *Eman M. Ibrahim, Lecturer of Nuclear Physics, Nuclear Materials Authority, Cairo, Egypt. E-mail: yousif_eman@yahoo.com*
- *Salwa Sewefi, Lecturer of Chemistry, Nuclear Materials Authority, Cairo, Egypt.*
- *Reda M. Attia, Assistant Lecturer of Chemistry, Nuclear Materials Authority, Cairo, Egypt. E-mail: chredamohamed@yahoo.com*

Radium exists in solution only in the divalent oxidation state. It is an unstable radioactive element found in a wide range of concentrations in all rocks, soil, and water. The natural decay series of three radionuclides (U, Th, and Ac) are the main sources of the four radium isotopes (^{226}Ra, ^{228}Ra, ^{224}Ra, and ^{223}Ra) in the environment [1].

Among radium isotopes ^{226}Ra is the most influential radionuclide due to its potential hazard to the environment, even at low concentrations [2]. Radium is only moderately soluble in water, and it enters ground water by dissolution of aquifer materials, by desorption from rock or sediment surfaces, and by ejection from minerals during radioactive decay.

In the U-series, the isotope of interest is ^{230}Th, rather than ^{232}Th, which is the parent of another natural decay series. The concentration and occurrence of ^{230}Th depends on its parent ^{234}U, although, chemically, it is reported to associate with refractory elements and the resistant fraction in sediments. ^{230}Th is a good indicator for nuclide migration in the ^{238}U series as it is immobile. The ^{226}Ra/^{238}U ratio is also a good indicator for alteration processes [3] and migration of either ^{238}U or ^{226}Ra according to the prevailing pH.

Radioactive decay leads to fractionation of radionuclides within the U-series. This process is known as the α-recoil effect (**Figure 1**) [4], [5]. Several studies have reviewed the α-recoil effect and its influence on fractionation of ^{238}U and ^{234}U in the environment [6], [7], [8], [9]. The parent ^{238}U decays to ^{234}Th by the emission of an alpha particle. As a result of momentum conservation, the daughter recoils to a distance in the range of 20-70 nm from the original position. The distribution of the parent nuclides in/on the grain and its surface significantly influence the release of daughter nuclides into solution. Following α-recoil, the product nuclide will be left in a disturbed crystal structure, due to local radiation damage. In an aqueous environment, water percolates into microfractures on the surfaces of mineral

grains, enhancing oxidation of ^{234}U to a higher oxidation state relative to ^{238}U. This leads to preferential release of ^{234}U from damaged lattice sites to solutions, and hence to disequilibrium [10]. The α-recoil phenomenon enhances not only the ^{234}U leaching but also the ^{230}Th and ^{228}Th [11].

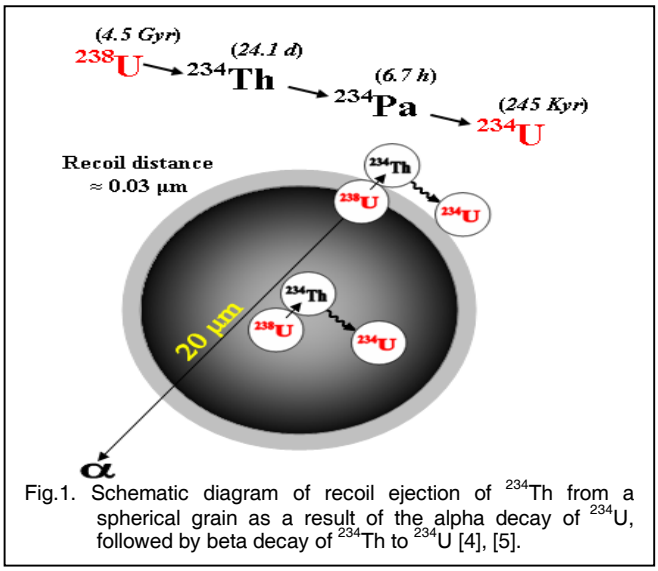

Fig.1. Schematic diagram of recoil ejection of ^{234}Th from a spherical grain as a result of the alpha decay of ^{234}U, followed by beta decay of ^{234}Th to ^{234}U [4], [5].

Uranium isotopes can dissolve from minerals and rocks and enter solution through chemical and physical processes. Physical processes involve α-recoil while chemical processes involve leaching through either acidic or alkaline reagents or any other leaching solution.

Chemical weathering of rocks is one of the major processes that modify the Earth's surface and is one of the vital processes in the geochemical distribution of elements. The rate and nature of chemical weathering are governed by many variables such as parent-rock type, topography, leaching conditions, and biological activity. The mobilization and redistribution of major and trace elements during weathering is particularly complicated because these elements are affected by various processes such as dissolution of primary minerals, formation of secondary phases, co-precipitation, and ion exchange on various minerals [12].

Laboratory experiments on chemical leaching of silicate minerals suggest that $^{234}U/^{238}U$ activity ratio disequilibria above unity can be generated in natural waters, due to preferential release of ^{234}U from damaged lattice sites [13], [14].

On sulfuric acid leaching of uranium ore, the results show that the uranium isotopes are leached to the same extent but the same is not observed for the other radionuclides [15].

Several recent studies that have focused on the analysis of U activity ratios [4], [16], [17], [18] consider the recoil ejection process to be the main cause of ^{234}U–^{238}U disequilibrium with the release rate of ^{234}U and ^{238}U during weathering to be identical.

Thus, observed fractionation between ^{234}U and ^{238}U is generally ascribed to selective leaching, α-recoil transfer of ^{234}Th directly into the aqueous phase, or a combination of the two processes. The principal aim of this work is to study radionuclide transfer from solid material (ore) to the liquid phase (leachate).

2 Geologic Setting

The sediments of the Um Bogma Formation at Allouga (**Figure 2**) are exposed 40 km east of Abu Zinema City in Sinai; the formation unconformably overlies the Adedia Formation (sandstones and shales), and is unconformably underlain by the non-fossiliferous bleached sandstones of the Abu Thora Formation. The lower and middle members of the Um Bogma Formation consist of carbonaceous black shale, sandy dolostone, limonitic marl, and siltstone, and are exposed in the face of Allouga Quarry and on the southeast side, with several mineralized layers.

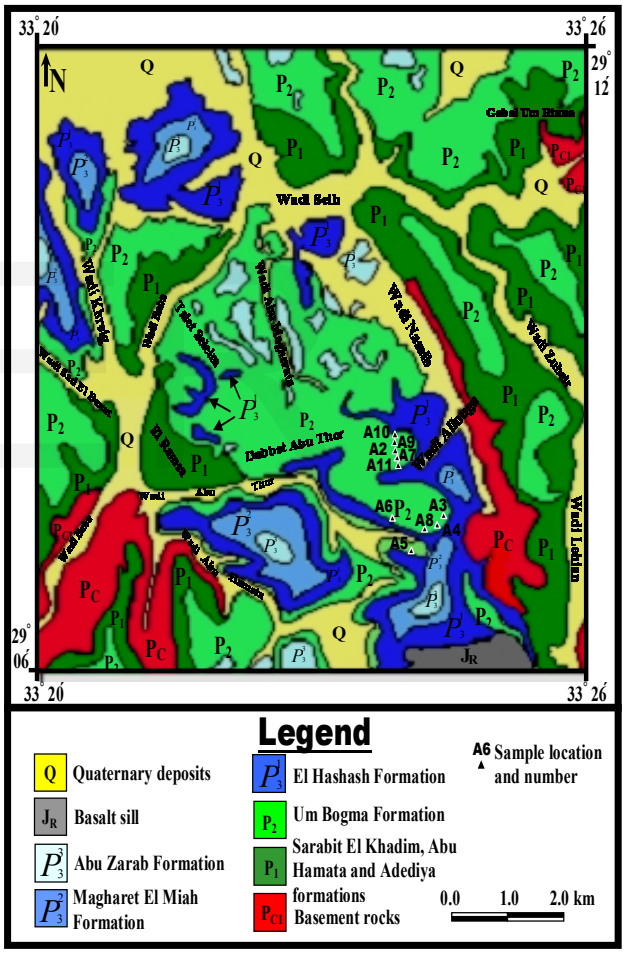

Fig. 2. Geologic map of the studied area [after El Aassy et al. [3] with modifications].

3 Experimental and Analytical Techniques

The selected samples were prepared for γ-ray spectrometric analysis by high purity germanium (HPGe) detector. The system has a relative efficiency of about 60% of the 3″ × 3″ NaI (Tl) crystal efficiency, a resolution of 2.3 keV, and peak/Compton ratio of 56:1 at the 1.33 MeV gamma transition of ^{60}Co. The system was calibrated for

energy to display gamma photopeaks between 46 keV and 3000 keV. The efficiency calibration was performed by using three well-known reference materials obtained from the International Atomic Energy Agency for U, Th, and K activity measurements: RGU-1, RGTh-1, and RGK-1 [19], [20].

^{238}U activity was determined indirectly from the γ-rays emitted by its daughter products (^{234}Th and ^{234m}Pa), whose activities are determined from the 63.3 and 1001 keV photopeaks, respectively [21]. ^{234}U activity was determined directly from the γ-rays emitted from this nuclide at energies of 53.2 keV and 120.9 keV [22], [23], [24]. To measure ^{230}Th activity, γ-ray emission at 67.7 keV was used [25]. The specific activity of ^{226}Ra was measured using the 186.1 keV from its own γ-ray (after the subtraction of the 185.7 keV of ^{235}U). ^{235}U activity was determined directly by γ-ray peaks: 143.8, 163.4, 185.7, and 205.3 keV [24], [26], [27]. The specific activity of ^{232}Th was measured using 338.4 keV and 911.2 keV from ^{228}Ac and 583 keV and 2614.4 keV from ^{208}Tl.

4 Sampling and Sample Preparation

Eleven samples were properly collected from Allouga, southwestern Sinai, Egypt. Theses samples were carefully described, crushed, ground to approximately (-60) mesh, and quartered to obtain representative samples for performing the experiments and analyses. About 200 ml of each sample was packed in a plastic container, weighed, then sealed and stored for four weeks to both prevent the escape of the radiogenic gases (^{222}Rn and ^{220}Rn) and allow the attainment of radioactive equilibrium in the decay chain. After the stored time the samples were measured for ^{238}U, ^{235}U, ^{234}U, ^{230}Th, ^{226}Ra, and ^{232}Th by HPGe. Each sample was measured during an accumulation time between 20 and 24 h. About 5 g of each sample was ground to -200 mesh (≈ 75 μm) for chemical analyses of major elements using Shapiro and Brannock's [28] technique.

5 Leaching Procedure

The measured samples were poured from the plastic containers and quartered to representative portions for leaching experiments using the acidic agitation technique with a magnetic stirrer. Each leaching experiment was performed by agitating 50 g of the ground sample with 150 ml acid of 200 g/l H_2SO_4 concentration for 1 h at room temperature. After the leaching process, the sample slurry was filtered and washed with distilled water several times and then made up to a volume of 250 ml. The leaching efficiency of the radionuclides was calculated according to the following equation:

$$\text{Leaching Efficiency}(\%) = \frac{\text{Activity concentration in the leachate}}{\text{Activity concentration in the original sample}} \times 100 \quad (1)$$

6 Results and Discussion

6.1 Sample Description

The collected samples represent the north face and southeast side of Gabal Allouga (**Figure 2**). The main rock types are sandstone, siltstone, shale, sandy dolostone, high-sulfur marl, and claystone. The main features of the collected samples are the dominating carbonate, iron, copper, and sulfur either as gypsum or in organic matter (O.M.) (**Table 1**).

Table 1. Chemical composition of different rock samples.

Sample Types	Dolostone				Marl		Claystone		Siltstone	Shale	Sandstone
Oxides %	A1	A2	A3	A4	A5	A6	A7	A8	A9	A10	A11
SiO_2	5.68	6.85	14.31	14.45	39.10	14.05	34.52	46.74	31.60	23.70	77.71
Al_2O_3	3.90	2.00	2.80	2.80	9.32	6.63	10.20	9.40	3.50	4.50	1.73
Fe_2O_3	11.70	1.60	4.80	4.80	6.52	3.55	5.25	27.90	4.72	5.50	4.79
CaO	17.00	24.50	12.60	15.40	6.53	6.40	3.27	1.40	13.30	17.00	4.20
MgO	15.12	15.70	20.15	18.10	8.62	13.34	2.65	2.02	8.30	9.20	3.00
Na_2O	2.10	0.38	0.88	0.81	0.11	0.12	0.70	0.10	0.27	0.26	0.03
K_2O	1.34	0.07	0.51	0.26	1.10	0.12	2.30	0.01	0.73	0.66	0.06
MnO	3.80	1.24	1.10	1.21	-	-	0.50	0.65	1.54	1.23	0.55
P_2O_5	0.68	1.02	1.16	1.19	0.15	0.09	0.76	1.52	0.42	0.55	0.62
TiO_2	0.50	0.15	0.08	0.06	0.37	0.30	1.57	1.45	0.53	0.81	1.23
CuO	0.72	0.15	3.59	1.35	0.14	8.89	0.68	0.56	0.50	0.50	0.59
Cl^-	2.30	0.43	0.37	0.35	0.18	0.18	2.70	0.18	0.74	0.64	0.46
SO_3^{-}	1.90	3.70	2.50	4.70	6.06	17.96	8.20	2.50	1.80	4.21	2.30
L.O.I	34.20	41.80	34.50	33.80	22.64	28.40	27.00	5.14	32.00	31.10	2.60
Total	100.94	99.59	99.35	99.28	99.74	100.03	100.30	99.57	99.95	99.86	99.87
O.M (450-550 °C)	2.47	1.86	2.80	2.80	4.30	2.96	2.56	2.80	3.60	3.06	0.14

6.2 Geochemical Characterization

Major element compositions of the analyzed samples are given in **Table 1**. From the obtained results, it can be concluded that the different rock types are mainly composed of SiO_2, CaO, MgO, Fe_2O_3, Al_2O_3, and SO_3 with average assays 28.06%, 11.10%, 10.56%, 7.38%, 5.16%, and 5.08%, respectively. Higher concentrations of CuO were observed in A3, A4, and A6 samples with assay 3.59%, 1.35%, and 8.89%, respectively, due to the presence of copper mineralization. The collected samples can be grouped according to high values of silicate, Al silicate, carbonate, and organic matter.

6.3 Radiometric Measurements

The activity concentrations of U- and Th-series nuclides in the studied sedimentary rocks are given in Table 2 along with some calculated isotopic ratios. The activity ratios of different radionuclides in different rock types (**Table 2 and Figure 3**) are clues for what happened in these rock varieties.

Table 2. Activity concentrations and activity ratios of radionuclides in original, leachate (pregnant solution), and residual samples.

Nuclide	Original (Bq/kg)		Pregnant Solution (Bq/ℓ)		(L %)	Residual (Bq/kg)	
A1 (Ferruginous Sandy Dolostone)							
^{238}U	3274.52	± 25.93	397.27	± 17.51	**12.13**	3309.90	± 51.53
^{234}U	2921.34	± 253.52	842.33	± 105.73	**28.83**	3535.41	± 269.57
^{230}Th	2170.57	± 50.24	98.21	± 31.68	**4.52**	1706.43	± 44.88
^{226}Ra	1913.67	± 5.96	16.81	± 0.88	**0.88**	1640.28	± 7.71
^{235}U	150.87	± 2.36	18.31	± 2.37	**12.13**	152.37	± 2.59
^{232}Th	25.03	± 0.65	5.91	± 0.35	**23.61**	29.12	± 0.91
^{238}U/^{235}U	21.70	± 0.51	21.70	± 3.77		21.72	± 0.71
^{234}U/^{235}U	19.36	± 1.98	46.02	± 11.74		23.20	± 2.16
^{234}U/^{238}U	0.89	± 0.08	2.12	± 0.36		1.07	± 0.10
^{230}Th/^{238}U	0.66	± 0.02	0.25	± 0.09		0.52	± 0.02
^{230}Th/^{234}U	0.74	± 0.08	0.12	± 0.05		0.48	± 0.05
^{226}Ra/^{238}U	0.58	± 0.01	0.04	± 0.004		0.50	± 0.01
^{226}Ra/^{230}Th	0.88	± 0.02	0.17	± 0.06		0.96	± 0.03
U (ppm)	***264.07***	***± 2.09***	***32.04***	***± 1.41***		***266.93***	***± 4.16***
Th (ppm)	***6.20***	***± 0.16***	***1.46***	***± 0.09***		***7.21***	***± 0.23***
A2 (Sandy Dolostone)							
^{238}U	2926.07	± 63.67	1869.41	± 97.62	**63.89**	1980.27	± 176.98
^{234}U	8451.34	± 300.93	4660.20	± 436.97	**55.14**	7979.95	± 791.49
^{230}Th	24651.40	± 134.10	10051.03	± 225.23	**40.77**	22615.67	± 394.30
^{226}Ra	22648.64	± 29.96	2563.40	± 20.20	**11.32**	20339.96	± 86.34
^{235}U	134.83	± 6.05	86.05	± 5.15	**63.82**	91.20	± 2.60
^{232}Th	11.89	± 1.12	2.25	± 0.17	**18.96**	8.78	± 1.63
^{238}U/^{235}U	21.70	± 1.45	21.73	± 2.43		21.71	± 2.56
^{234}U/^{235}U	62.68	± 5.05	54.16	± 8.32		87.50	± 11.18
^{234}U/^{238}U	2.89	± 0.17	2.49	± 0.36		4.03	± 0.76
^{230}Th/^{238}U	8.42	± 0.23	5.38	± 0.40		11.42	± 1.22
^{230}Th/^{234}U	2.92	± 0.12	2.16	± 0.25		2.83	± 0.33
^{226}Ra/^{238}U	7.74	± 0.18	1.37	± 0.08		10.27	± 0.96
^{226}Ra/^{230}Th	0.92	± 0.01	0.26	± 0.008		0.90	± 0.02
U (ppm)	***235.97***	***± 5.13***	***150.76***	***± 7.87***		***159.70***	***±14.27***
Th (ppm)	***2.94***	***± 0.28***	***0.56***	***± 0.04***		*2.17*	*± 0.40*
A3 (Sandy Dolostone)							
^{238}U	2778.03	± 22.83	1097.07	± 43.81	**39.49**	1681.54	± 43.15
^{234}U	1670.31	± 138.24	1431.23	± 381.34	**85.69**	691.76	± 36.96
^{230}Th	2986.53	± 63.78	537.67	± 92.94	**18.00**	2291.45	± 86.48
^{226}Ra	2966.09	± 8.29	311.40	± 5.22	**10.50**	2681.46	± 16.71
^{235}U	127.78	± 2.71	50.52	± 3.12	**39.54**	77.44	± 4.15
^{232}Th	28.88	± 1.20	3.96	± 0.23	**13.70**	27.87	± 1.45
^{238}U/^{235}U	21.74	± 0.64	21.71	± 2.21		21.71	± 1.72
^{234}U/^{235}U	13.07	± 1.36	28.33	± 9.30		8.93	± 0.96
^{234}U/^{238}U	0.60	± 0.05	1.30	± 0.40		0.41	± 0.03
^{230}Th/^{238}U	1.08	± 0.03	0.49	± 0.10		1.36	± 0.09
^{230}Th/^{234}U	1.79	± 0.19	0.38	± 0.17		3.31	± 0.30
^{226}Ra/^{238}U	1.07	± 0.01	0.28	± 0.02		1.59	± 0.05
^{226}Ra/^{230}Th	0.99	± 0.02	0.58	± 0.11		1.17	± 0.05
U (ppm)	***224.03***	***± 1.84***	***88.47***	***± 3.53***		***135.61***	***± 3.48***
Th (ppm)	***7.15***	***± 0.30***	***0.98***	***± 0.06***		***6.90***	***± 0.36***

Nuclide	Original (Bq/kg)		Pregnant Solution (Bq/ℓ)		(L %)	Residual (Bq/kg)	
A4 (Sandy Dolostone)							
^{238}U	1849.86	± 17.61	527.12	± 25.76	**28.50**	1330.63	± 33.26
^{234}U	1431.17	± 121.68	1031.13	± 306.43	**72.05**	724.76	± 132.79
^{230}Th	1555.48	± 38.32	248.54	± 85.86	**15.98**	1157.56	± 60.35
^{226}Ra	1007.23	± 4.07	167.91	± 3.52	**16.67**	819.84	± 8.40
^{235}U	85.18	± 1.90	24.28	± 2.82	**28.50**	61.29	± 2.72
^{232}Th	26.84	± 0.83	4.49	± 0.39	**16.73**	23.86	± 1.30
^{238}U/^{235}U	21.72	± 0.69	21.71	± 3.59		21.71	± 1.51
^{234}U/^{235}U	16.80	± 1.80	42.47	± 17.56		11.83	± 2.69
^{234}U/^{238}U	0.77	± 0.07	1.96	± 0.68		0.54	± 0.11
^{230}Th/^{238}U	0.84	± 0.03	0.47	± 0.19		0.87	± 0.07
^{230}Th/^{234}U	1.09	± 0.12	0.24	± 0.15		1.60	± 0.38
^{226}Ra/^{238}U	0.54	± 0.01	0.32	± 0.02		0.62	± 0.02
^{226}Ra/^{230}Th	0.65	± 0.02	0.68	± 0.25		0.71	± 0.04
U (ppm)	***149.18***	***± 1.42***	***42.51***	***± 2.08***		***107.31***	***± 2.68***
Th (ppm)	***6.64***	***± 0.21***	***1.11***	***± 0.10***		***5.91***	***± 0.32***
A5 (Ferruginous Carbonaceous Marl)							
^{238}U	14737.73	± 181.39	11309.05	± 113.76	**76.74**	3384.32	± 137.51
^{234}U	23736.62	± 2330.90	19279.96	± 1487.34	**81.22**	4599.70	± 736.94
^{230}Th	23672.77	± 557.57	3421.53	± 104.89	**14.45**	18672.23	± 246.95
^{226}Ra	15697.78	± 66.36	1211.89	± 10.05	**7.72**	14915.62	± 43.41
^{235}U	678.26	± 21.93	520.83	± 6.96	**76.79**	155.95	± 7.14
^{232}Th	60.31	± 4.79	3.49	± 0.31	**5.79**	61.03	± 3.35
^{238}U/^{235}U	21.73	± 0.97	21.71	± 0.51		21.70	± 1.88
^{234}U/^{235}U	35.00	± 4.57	37.66	± 3.39		29.49	± 6.08
^{234}U/^{238}U	1.61	± 0.18	1.73	± 0.15		1.36	± 0.27
^{230}Th/^{238}U	1.61	± 0.06	0.30	± 0.01		5.52	± 0.30
^{230}Th/^{234}U	1.00	± 0.12	0.17	± 0.02		4.06	± 0.70
^{226}Ra/^{238}U	1.07	± 0.02	0.11	± 0.002		4.41	± 0.19
^{226}Ra/^{230}Th	0.66	± 0.02	0.35	± 0.01		0.80	± 0.01
U (ppm)	***1188.53***	***± 14.63***	***912.02***	***± 9.17***		***272.93***	***± 11.09***
Th (ppm)	***14.93***	***± 1.19***	***0.86***	***± 0.08***		***15.11***	***± 0.83***
A6 (High Sulfur Marl)							
^{238}U	14514.52	± 268.66	13615.52	± 259.32	**93.81**	3118.80	± 77.48
^{234}U	10991.32	± 1561.23	10585.25	± 1143.36	**96.31**	1211.09	± 56.75
^{230}Th	9055.57	± 688.14	2726.38	± 227.02	**30.11**	4507.17	± 165.50
^{226}Ra	9304.89	± 64.53	3164.29	± 26.03	**34.01**	7743.40	± 32.52
^{235}U	668.51	± 23.37	627.10	± 14.80	**93.81**	143.53	± 6.36
^{232}Th	15.16	± 3.87	1.63	± 0.18	**10.77**	16.83	± 1.62
^{238}U/^{235}U	21.71	± 1.16	21.71	± 0.93		21.73	± 1.50
^{234}U/^{235}U	16.44	± 2.91	16.88	± 2.22		8.44	± 0.77
^{234}U/^{238}U	0.76	± 0.12	0.78	± 0.10		0.39	± 0.03
^{230}Th/^{238}U	0.62	± 0.06	0.20	± 0.02		1.45	± 0.09
^{230}Th/^{234}U	0.82	± 0.18	0.26	± 0.05		3.72	± 0.31
^{226}Ra/^{238}U	0.64	± 0.02	0.23	± 0.01		2.48	± 0.07
^{226}Ra/^{230}Th	1.03	± 0.09	1.16	± 0.11		1.72	± 0.07
U (ppm)	***1170.53***	***± 21.67***	***1098.03***	***± 20.91***		***251.52***	***± 6.25***
Th (ppm)	***3.75***	***± 0.96***	***0.40***	***± 0.04***		***4.17***	***± 0.40***

Table 2. Continue.

Nuclide	Original (Bq/kg)		Pregnant Solution (Bq/l)		(L %)	Residual (Bq/kg)	
A7 (High-Sulfur Ferruginous Claystone)							
^{238}U	4894.69	± 32.82	2611.11	± 52.98	**53.35**	2395.98	± 54.37
^{234}U	3548.83	± 228.81	3318.36	± 444.85	**93.51**	1962.13	± 301.5
^{230}Th	2342.56	± 76.30	169.55	± 40.15	**7.24**	1892.59	± 93.73
^{226}Ra	1651.37	± 6.18	16.09	± 0.31	**0.97**	1842.97	± 13.80
^{235}U	225.24	± 3.15	120.26	± 4.66	**53.39**	110.25	± 4.55
^{232}Th	92.82	± 1.77	1.84	± 0.15	**1.98**	94.54	± 2.60
^{238}U/^{235}U	21.73	± 0.45	21.71	± 1.28		21.73	± 1.39
^{234}U/^{235}U	15.76	± 1.24	27.59	± 4.77		17.80	± 3.47
^{234}U/^{238}U	0.73	± 0.05	1.27	± 0.20		0.82	± 0.14
^{230}Th/^{238}U	0.48	± 0.02	0.06	± 0.02		0.79	± 0.06
^{230}Th/^{234}U	0.66	± 0.06	0.05	± 0.02		0.96	± 0.20
^{226}Ra/^{238}U	0.34	± 0.004	0.006	± 0.0002		0.77	± 0.02
^{226}Ra/^{230}Th	0.70	± 0.03	0.09	± 0.02		0.97	± 0.06
U (ppm)	***394.73***	***± 2.65***	***210.57***	***± 4.27***		***193.22***	***± 4.38***
Th (ppm)	***22.97***	***± 0.44***	***0.45***	***± 0.04***		***23.40***	***± 0.64***
A8 (Highly Ferruginous Claystone)							
^{238}U	239.62	± 7.35	144.05	± 11.80	**60.12**	177.13	± 17.55
^{234}U	183.07	± 108.39	164.28	± 68.61	**89.74**	78.40	± 16.20
^{230}Th	267.32	± 20.64	96.44	± 27.56	**36.08**	182.29	± 33.07
^{226}Ra	255.08	± 2.50	12.11	± 0.59	**4.75**	265.68	± 4.67
^{235}U	11.03	± 0.93	6.63	± 0.88	**60.11**	8.15	± 0.55
^{232}Th	94.90	± 1.07	2.75	± 0.17	**2.89**	116.10	± 3.10
^{238}U/^{235}U	21.72	± 2.49	21.72	± 4.68		21.74	± 3.63
^{234}U/^{235}U	16.59	± 11.22	24.78	± 13.65		9.62	± 2.64
^{234}U/^{238}U	0.76	± 0.48	1.14	± 0.57		0.44	± 0.14
^{230}Th/^{238}U	1.12	± 0.12	0.67	± 0.25		1.03	± 0.29
^{230}Th/^{234}U	1.46	± 0.98	0.59	± 0.41		2.33	± 0.90
^{226}Ra/^{238}U	1.06	± 0.04	0.08	± 0.01		1.50	± 0.18
^{226}Ra/^{230}Th	0.95	± 0.08	0.13	± 0.04		1.46	± 0.29
U (ppm)	***19.32***	***± 0.59***	***11.62***	***± 0.95***		***14.29***	***± 1.42***
Th (ppm)	***23.49***	***± 0.27***	***0.68***	***± 0.04***		***28.74***	***± 0.77***
A9 (Calcareous Siltstone)							
^{238}U	13694.94	± 59.99	7644.27	± 123.47	**55.82**	7505.49	± 169.2
^{234}U	9556.60	± 918.16	6115.80	± 977.04	**64.00**	5486.35	± 1619
^{230}Th	9370.70	± 69.43	2479.99	± 89.52	**26.47**	7067.00	±123.72
^{226}Ra	9490.49	± 13.71	430.17	± 4.92	**4.53**	9854.22	± 34.06
^{235}U	630.61	± 5.90	352.14	± 5.06	**55.84**	345.51	± 8.52
^{232}Th	38.72	± 1.49	3.82	± 0.25	**9.88**	35.24	± 1.99
^{238}U/^{235}U	21.72	± 0.30	21.71	± 0.66		21.72	± 1.03
^{234}U/^{235}U	15.15	± 1.60	17.37	± 3.02		15.88	± 5.08
^{234}U/^{238}U	0.70	± 0.07	0.80	± 0.14		0.73	± 0.23
^{230}Th/^{238}U	0.68	± 0.01	0.32	± 0.02		0.94	± 0.04
^{230}Th/^{234}U	0.98	± 0.10	0.41	± 0.08		1.29	± 0.40
^{226}Ra/^{238}U	0.69	± 0.004	0.06	± 0.002		1.31	± 0.03
^{226}Ra/^{230}Th	1.01	± 0.01	0.17	± 0.01		1.39	± 0.03
U (ppm)	***1104.43***	***± 4.84***	***616.47***	***± 9.96***		***605.28***	***± 13.64***
Th (ppm)	***9.58***	***± 0.37***	***0.95***	***± 0.06***		***8.72***	***± 0.49***

Nuclide	Original (Bq/kg)		Pregnant Solution (Bq/l)		(L %)	Residual (Bq/kg)	
A10 (Calcareous Shale)							
^{238}U	1493.18	± 16.58	845.02	± 34.64	**56.59**	765.35	± 26.01
^{234}U	1350.15	± 140.61	1415.83	± 331.44	**104.86**	958.69	± 69.55
^{230}Th	818.44	± 63.08	159.77	± 50.87	**19.52**	777.60	± 63.33
^{226}Ra	990.94	± 4.77	31.50	± 0.76	**3.18**	988.65	± 10.68
^{235}U	68.76	± 1.59	38.90	± 3.91	**56.57**	35.22	± 3.35
^{232}Th	41.43	± 1.01	6.40	± 0.69	**15.45**	46.63	± 1.86
^{238}U/^{235}U	21.72	± 0.74	21.72	± 3.07		21.73	± 2.81
^{234}U/^{235}U	19.64	± 2.50	36.40	± 12.18		27.22	± 4.56
^{234}U/^{238}U	0.90	± 0.10	1.68	± 0.46		1.25	± 0.13
^{230}Th/^{238}U	0.55	± 0.05	0.19	± 0.07		1.02	± 0.12
^{230}Th/^{234}U	0.61	± 0.11	0.11	± 0.06		0.81	± 0.12
^{226}Ra/^{238}U	0.66	± 0.01	0.04	± 0.002		1.29	± 0.06
^{226}Ra/^{230}Th	1.21	± 0.10	0.20	± 0.07		1.27	± 0.12
U (ppm)	***120.42***	***± 1.34***	***68.15***	***± 2.79***		***61.72***	***± 2.10***
Th (ppm)	***10.25***	***± 0.25***	***1.58***	***± 0.17***		***11.54***	***± 0.46***
A11 (Sandstone)							
^{238}U	172.06	± 8.31	82.95	± 6.92	**48.21**	95.87	± 10.45
^{234}U	166.20	± 11.57	195.51	± 75.70	**117.63**	70.28	± 16.82
^{230}Th	175.85	± 27.12	111.59	± 26.51	**63.46**	113.06	± 24.03
^{226}Ra	142.85	± 1.78	29.82	± 1.22	**20.88**	150.39	± 4.06
^{235}U	7.92	± 0.66	3.82	± 0.48	**48.23**	4.41	± 0.35
^{232}Th	22.18	± 0.58	2.28	± 0.16	**10.26**	23.95	± 1.19
^{238}U/^{235}U	21.71	± 2.86	21.72	± 4.55		21.73	± 4.12
^{234}U/^{235}U	20.97	± 3.21	51.18	± 26.27		15.93	± 5.09
^{234}U/^{238}U	0.97	± 0.11	2.36	± 1.11		0.73	± 0.26
^{230}Th/^{238}U	1.02	± 0.21	1.35	± 0.43		1.18	± 0.38
^{230}Th/^{234}U	1.06	± 0.24	0.57	± 0.36		1.61	± 0.73
^{226}Ra/^{238}U	0.83	± 0.05	0.36	± 0.04		1.57	± 0.21
^{226}Ra/^{230}Th	0.81	± 0.14	0.27	± 0.07		1.33	± 0.32
U (ppm)	***13.88***	***± 0.67***	***6.69***	***± 0.56***		***7.73***	***± 0.84***
Th (ppm)	***5.49***	***± 0.14***	***0.56***	***± 0.04***		***5.93***	***± 0.29***

^{238}U in the ferruginous sandy dolostone (A1) and sandy dolostone (A2, A3, and A4) samples exhibited a large variation of 149.18 to 264.07 ppm, as well as a relatively wide range of ^{232}Th from 2.94 to 7.15 ppm. In contrast, high-sulfur marl and ferruginous carbonaceous marl samples (A5 and A6) had ^{238}U concentrations of 1188.53 and 1170.53 ppm and ^{232}Th concentrations of 14.93 and 3.75 ppm, respectively. This disparity in radionuclide content may reflect different source terms, as well as varying associations with secondary minerals and organic matter content [29].

The ^{232}Th/^{238}U activity ratios were 0.02 in the ferruginous sandy dolostone (A1), 0.01, 0.03 and 0.04 in the sandy dolostone (A2, A3, and A4), 0.003 in the high-sulfur marl (A6), and 0.01 in the ferruginous carbonaceous marl (A5).

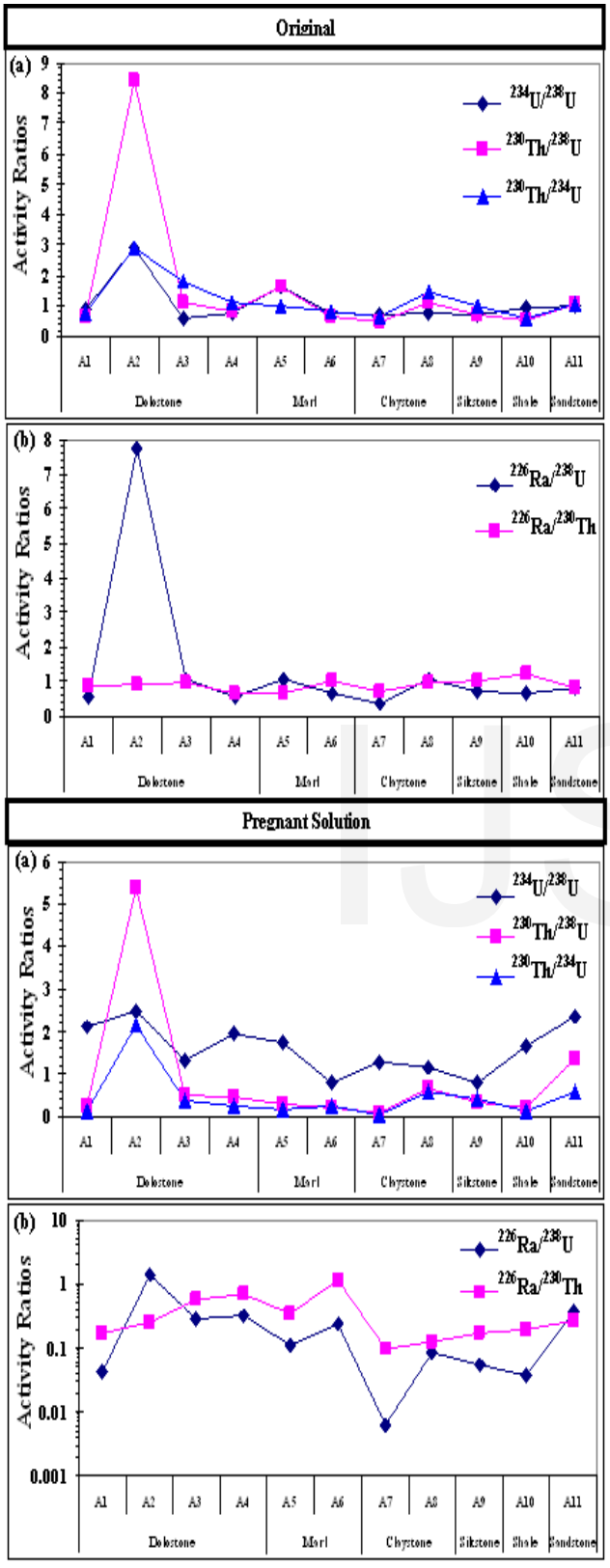

Fig. 3. Variations of the (a) $^{234}U/^{238}U$, $^{230}Th/^{238}U$ and $^{230}Th/^{234}U$ and (b) $^{226}Ra/^{238}U$ and $^{226}Ra/^{230}Th$ activity ratios in original, pregnant solution and residual samples.

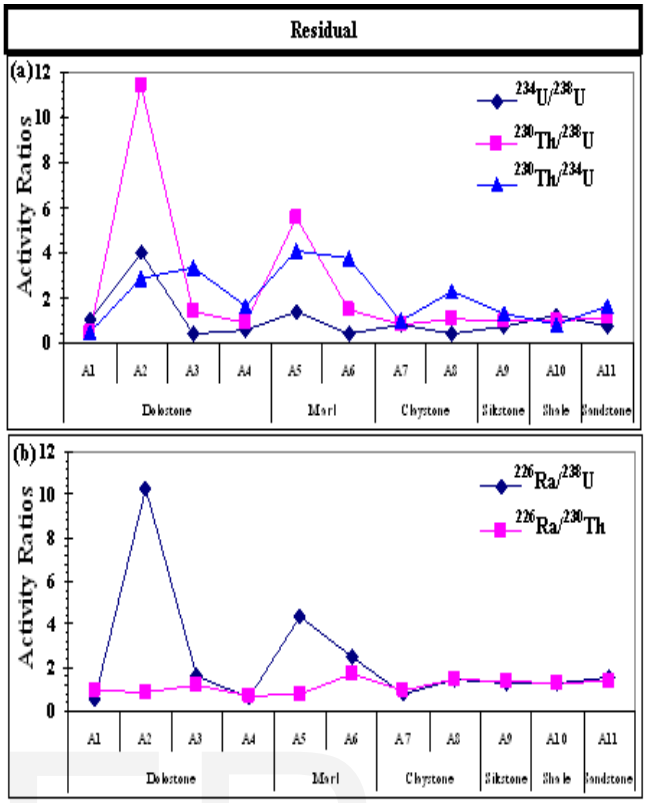

Fig. 3. Continue.

$^{232}Th/^{238}U$ activity ratios in calcareous siltstone (A9), calcareous shale (A10), calcareous sandstone (A11), high sulfoferruginous claystone (A7), and highly ferruginous claystone (A8) were 0.009, 0.09, 0.40, 0.06, and 1.22, respectively, all of which are much lower than typical values of 3 to 4 for the Earth's crust [30], indicating uranium enrichment in these samples.

Figure 3 demonstrates that the $^{230}Th/^{238}U$, $^{230}Th/^{234}U$, $^{226}Ra/^{238}U$, and $^{234}U/^{238}U$ activity ratios for all studied samples deviate significantly from equilibrium. These activity ratios are consistent with the preferential mobilization of uranium from the studied samples by leaching.

The $^{234}U/^{238}U$ activity ratios are less than 1 for all rock samples except A2 and A5, indicating preferential mobilization of ^{234}U relative to ^{238}U from the rock due to prevailing oxidizing conditions (**Figure 3**). The higher activity ratio measured in the sandy dolostone (A2) and marl sample (A5) may be related to its presence within the oxic-anoxic transition subzone resulting in enrichment of ^{234}U and ^{230}Th relative to ^{238}U in a reducing environment. Generally, weathered rocks deviate from secular equilibrium due to differences in radionuclide mobility during weathering processes. This relative mobility is believed to be $^{234}U>^{238}U>^{230}Th$, and consequently weathered rocks are assumed to have $^{234}U/^{238}U<1$ and $^{230}Th/^{238}U>1$ [5], [8], [31]. Disequilibrium among ^{238}U-^{234}U-^{230}Th in A1, A2,

A3, and A4 is an indication of the role of chemical weathering in these samples resulting from the preferential solubility of these isotopes. The observation of whether $^{234}U/^{238}U$ activity ratios are less than or greater than 1 can show that isotopes of uranium have migrated within the rock in the last 1 to 2 million years; the time required for ^{234}U to reach its equilibrium activity [32]. Other daughter/parent activity ratios can be used to detect radionuclide migration over shorter time-scales, such as $^{230}Th/^{238}U$ (300,000 years; the time required for ^{230}Th to reach its equilibrium activity if $^{234}U/^{238}U$ activity ratio is 1) and $^{226}Ra/^{230}Th$ (8,000 years; the time required for ^{226}Ra to reach its equilibrium activity with ^{230}Th).

$^{230}Th/^{238}U$ activity ratios <1 in samples A1, A4, A6, A7, A9, and A10 can be ascribed to preferential uranium accumulation, while in A3, A8, and A11 are 1.08, 1.12, and 1.02, which shows an equilibrium state (**Figure 3**). Sample A2 shows $^{230}Th/^{238}U$ and $^{230}Th/^{234}U$ activity ratios >1 indicating preferential uranium leaching in an oxidizing environment. The results of Sarin et al. [33] on ^{230}Th excess over ^{238}U in the Ganga River suspended sediments attest to preferential mobility of U over Th during weathering. Selective extraction studies show secondary iron minerals retard migration of U and particularly Th isotopes [34]. Excess ^{230}Th in sample A5, could be either due to U loss from the sample or ^{230}Th gain resulting from recoil-implanted ^{230}Th atoms from decay of ^{234}U atoms dissolved in solution as suggested by Lowson et al. [35] and Mathieu et al. [36]. Taking into account the geochemical immobility of Th can explain why some solids show $^{234}U/^{238}U$ and $^{230}Th/^{238}U$ activity ratios greater than unity. This process is called $^{234}U + ^{230}Th$ recoil gain at solid-liquid interface.

The activity ratios of $^{226}Ra/^{238}U$ increased from 0.34 to 7.74 (**Figure 3**) which may related to the fact that radium appeared to be relatively mobile in the more reducing condition [37], [38]. The decrease of ^{226}Ra solubility can be caused by co-precipitation with $(Ba,Pb)SO_4$ [39]. Saad et al. [40] found that Mn-ore deposits in the Um Bogma region are enriched in Pb, Cu, Zn, and Ba indicating that ^{226}Ra may co-precipitate with lead and barium sulfates. Also, dug and drilled wells in these rocks indicate that the underground water contains high Cl^- and SO_4^{2-} concentrations [41].

El Aassy et al. [3] revised uranium migration processes in dolostones to dedolomitization while karstification and lateritization led to migration of uranium from shales, siltstones, and claystones. These alteration processes play an important role in disruption of these isotopic ratios.

The $^{226}Ra/^{230}Th$ activity ratio is significantly different from unity in sample A10 (1.2). This could be attributed to the promotion of ^{230}Th solubility by forming complexes with Cl^- or SO_4^{2-} ions (e.g., $[ThCl_3]^+$ and $[ThSO_4]^{2+}$) [42], indicating the system was not closed to surface and groundwater movement for a maximum time period of 8 ky.

Until very recently it was assumed that the current $^{238}U/^{235}U$ ratio was a constant value (21.7) in our Solar System because uranium was thought to be too heavy to undergo significant isotope fractionation. Theoretical work by Fujii et al. [43], Bigeleisen [44], and Schauble [45], [46] suggested, however, that fractionation in uranium isotopes should be present and measurable with modern analytical techniques. Recent work has in fact shown variability in the terrestrial $^{238}U/^{235}U$ ratio over a range of ~1.3‰ [47].

The $^{238}U/^{235}U$ activity ratios of the studied rocks varied between 21.70 and 21.74 with 21.72 as an average (**Figure 4**), suggesting that redox played an important role in fractionation of ^{238}U and ^{235}U [47], [48], [49]. Theoretically, ^{235}U was preferentially retained in oxidized species such as dissolved U^{6+}, whereas ^{238}U was preferentially partitioned into reduced species such as uraninite [44], [45].

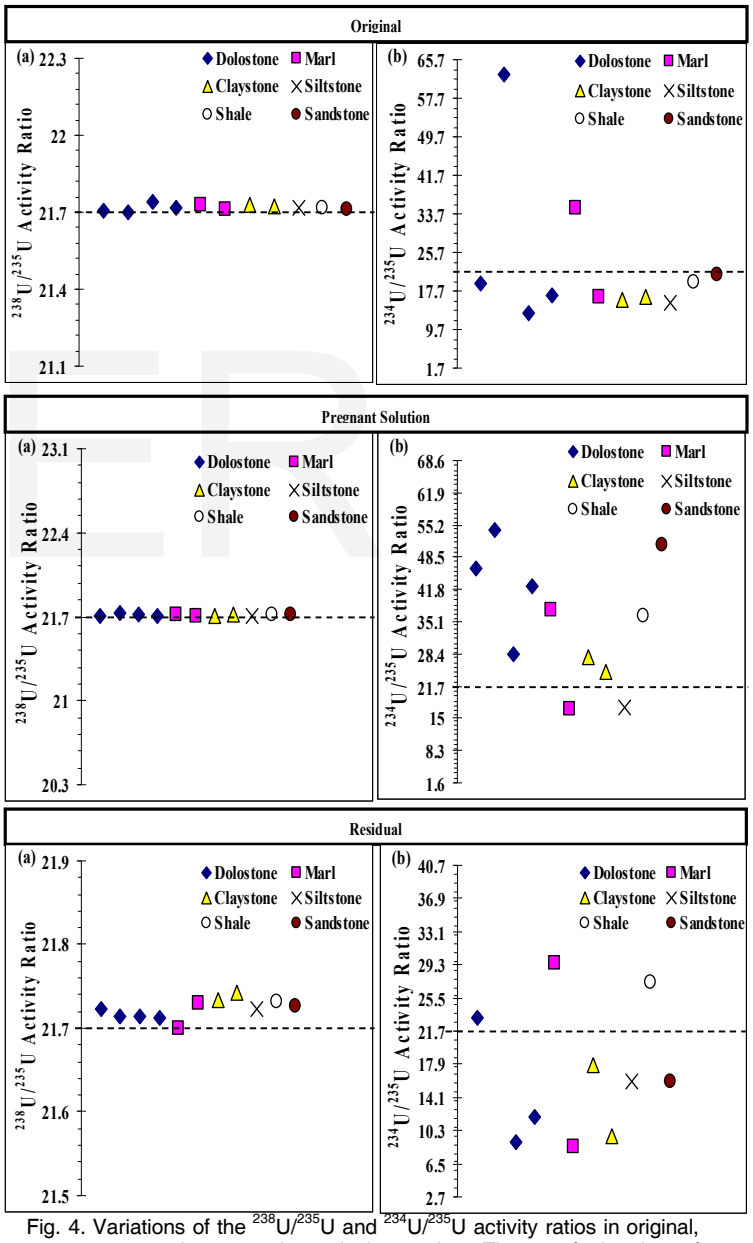

Fig. 4. Variations of the $^{238}U/^{235}U$ and $^{234}U/^{235}U$ activity ratios in original, pregnant solution, and residual samples. The certified value of $^{238}U/^{235}U$ activity ratio is 21.7, which is shown with the dashed lines.

Although significant variations in the $^{238}U/^{235}U$ ratio have been recently discovered, much larger variations in

the $^{234}U/^{235}U$ ratio in the terrestrial variations have long been observed [47]. In contrast to the values of $^{238}U/^{235}U$ ratios, the $^{234}U/^{235}U$ ratios in the studied rocks range between 13.07 and 62.68, indicating ^{234}U leaching due to alteration processes (**Figure 4**).

6.4 Leaching Experiments

Leaching experiments on different sedimentary rock types were performed under conditions that approximated natural conditions, with the aim of determining the effect of physical and chemical processes on the mobility of U- and Th-series nuclides (**Table 2**).

The leaching data show elemental and isotopic fractionations. Whereas the incongruent dissolution of uranium and thorium may be explained by chemical effects, the fractionations upon dissolution among the three uranium isotopes and among the two thorium isotopes is inconsistent with chemical kinetics if the nuclides are dissolved from the same solid phase [50].

Sulfuric acid leaching experiments of the studied ferruginous sandy dolostone (A1) and sandy dolostone (A2, A3, and A4) samples leached from 12.13 to 63.89% of ^{238}U, 12.13 to 63.82% of ^{235}U, 28.83 to 85.69% of ^{234}U, 4.52 to 40.52% of ^{230}Th, and 0.88 to 16.67% of ^{226}Ra. The low leachability for most radionuclides is due to acid consumption by carbonates (**Figure 5**). Benes et al. [51] suggest the maximum value of $CaCO_3$ cannot exceed 5% as that might cause chemical colmatation of the ore bedding during leaching processes. Several studies have shown that carbonate concentration in leaching solutions, among other factors, may influence uranium extraction and leaching from ore and soils [42], [52], [53]. The lowest value of leachability was recorded in sample A1; this may be related to the presence of iron minerals. Payne and Airey [54] inferred from the mineralogical studies of Koongarra samples that adsorption on iron minerals, and subsequent post-adsorption processes, were extremely important in the long-term immobilization of U in the system and supported their conclusion by laboratory investigations of the relative importance of iron oxides in uranium adsorption. Payne et al. [55] found that the chemical removal of iron minerals from Koongarra samples leads to significant decreases in their ability to adsorb uranium. In the dispersion fan, adsorption of U (VI) on Fe-oxides and clays appears to play a major role in reducing U mobility [54], [56].

The highest leachability values for ^{234}U and ^{230}Th were found in the calcareous sandstone sample A11, where they reached 117.63% and 63.46%, respectively (**Figure 5**). The highest leachability values for ^{238}U, ^{235}U, and ^{226}Ra were found in the high-sulfur marl sample A6 assaying 93.81%, 93.81%, and 34.01%, respectively. These values were also high in the ferruginous marl sample A5. In both samples, the high leachability could be ascribed to high contents of SO_3^{--} which may increase acid concentration and enhance leachability.

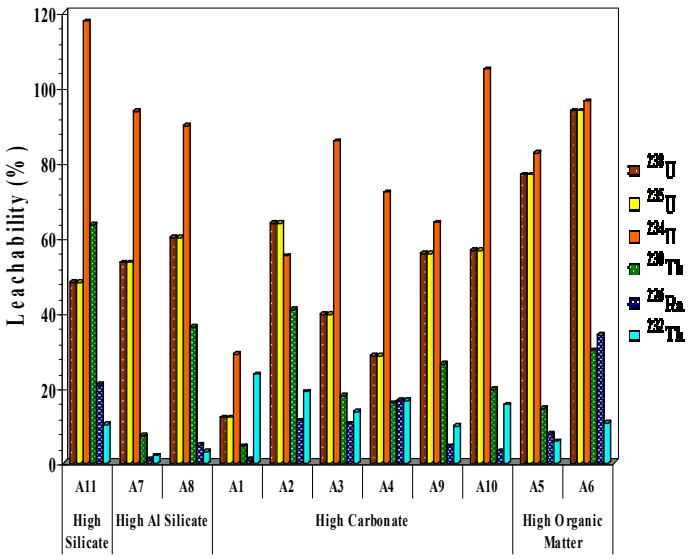

Fig. 5. Leaching efficiency (%) of different radionuclides.

Singh et al. [57] stated that many organic-rich sediments contain pyrite, the oxidation of which produces H_2SO_4 which can enhance chemical weathering. Microbial oxidation of accessory pyrite can lead to comparable recoveries of U, Y, and rare earth elements and in effect make the ore 'self-leaching.' Previous studies recorded the presence of framboidal pyrite in the studied area suggesting microorganisms may play a role.

Nearly identical values of leachability were recorded for ^{238}U and ^{235}U (**Figure 5**). This observation was previously recorded by Ibrahim [58].

Chabaux et al. [8] showed that the leaching efficiency for ^{234}U and ^{238}U are identical and this supports the high leaching efficiency for ^{234}U which reached 96.31%, 101.44%, and 117.63% in samples A6, A10, and A11, respectively, due to α-recoil which is significant only when the grain size is sufficiently small or the surface area contact with percolating fluids is large.

The activity ratio $^{234}U/^{238}U$ >1 in all leachate samples except samples A6 and A9 (**Figure 3**) may be due to preferential dissolution of ^{234}U from tracks produced by α-recoil atoms of ^{234}U during the leaching period. These lines of severe crystal damage are more readily chemically attacked by the etchant/leachant than the undamaged or naturally annealed crystal sites, in which most of the ^{238}U atoms reside. The leaching process has therefore removed ^{234}U preferentially from ores, so that the activity ratios of $^{234}U/^{238}U$ are greater than 1. The lower $^{234}U/^{238}U$ activity ratios in leachate of the marl sample (A6) and siltstone sample (A9) may be attributed to the presence of these uranium radionuclides (^{234}U and ^{238}U) as weakly adsorbed surficial uranyl compounds in marl rocks leading to identical activities in both the original sample and pregnant solution.

The above arguments may explain the enrichment of ^{234}U relative to that of its ancestor nuclide, the structurally

incorporated isotope ^{238}U. Under undisturbed and steady conditions, equilibrium would be expected between the activity concentration of ^{238}U and ^{234}U; however, this is not always the case. According to Bourdon et al. [7], Adloff and Rössler [59], Suksi et al. [60], and Satybaldiyev et al. [61], the reasons for $^{234}U/^{238}U$ activity ratio disequilibrium are (1) recoil effect, which induces ejection of decay product from a particle into its environment, and (2) increased mobility of a decay product due to subsequent oxidation of ^{234}U in zones which are not close to the phase boundary.

On the other hand, the activity ratios of $^{230}Th/^{234}U < 1$ in the leachate for all samples (**Figure 3**) result from preferential dissolution of ^{234}U from the original (ore sample) into the pregnant solution [62]. $^{230}Th/^{238}U$ activity ratios are slightly greater than 1 only in one sample (A11) and highly greater than unity in sample (A2); this probably results from the leaching of U that would be fixed again (adsorption) to the solid phase (residual). Re-precipitation of mobilized and reduced ^{238}U (IV) from the pregnant solution would result in $^{230}Th/^{238}U$ activity ratios <1 (**Figure 3**). Bacteria and fungi are thought to be responsible for uranium reduction and precipitation [63].

Nuclides in the α-recoil track may have higher reactivity with fluid, leading to their preferential fractionation during acid leaching if the track has not been sufficiently annealed. Thus, the following three hypotheses can be considered to explain the ^{238}U–^{230}Th disequilibria for both the leachate and the residue [64], [65]; (a) a redistribution of ^{234}Th and/or ^{230}Th caused by α-recoil between the acid-soluble and acid-resistant phases after solidification, (b) the preferential dissolution of nuclides reorganized by α-recoil during acid leaching, and (c) the preferential U/Th fractionation by incongruent dissolution of phases during acid leaching.

The $^{226}Ra/^{238}U$ and $^{226}Ra/^{230}Th$ activity ratios were below unity in most samples (**Figure 3**), which may suggest that U- and Th-fixing is the main process responsible for lowering these ratios. The $^{226}Ra/^{230}Th$ ratio exceeded unity in one sample (A6); this result could indicate that ^{226}Ra is quite mobile relative to ^{230}Th in this sample. The observed $^{226}Ra/^{238}U$ activity ratios could be attributed to differences in geochemistry of the two isotopes. Uranium mobility is redox-sensitive because the dominant oxidation state of uranium under reducing conditions is U (IV) which is relatively insoluble and immobile, whereas under oxidizing conditions mobile U (VI) species are present. In contrast, radium only has the one oxidation state (II), and is immobilized by co-precipitation and solid solution formation of radium in divalent metal sulfate and carbonate minerals [66], [67], and by adsorption on other minerals. Radium generally has an intermediate mobility between U (IV) and U (VI), but, in contrast to uranium, is less mobile in oxidizing conditions because it is strongly adsorbed by clay and iron minerals [68], [69], which are often present in oxidizing conditions and arise from weathering of the host rock [70], [37], [38].

A significant difference in $^{238}U/^{235}U$ ratios (**Figure 4**) may be related to an oxidation-reduction condition prevailing during the leaching processes. There is a growing body of evidence suggesting that the leaching of uranium during low-temperature weathering preferentially releases the light ^{235}U isotope and leaves the heavier ^{238}U in the residue. Further, leaching experiments of euxenite show evidence of ^{235}U enrichment in leachate [71], [72].

The samples show diverse results in the $^{234}U/^{235}U$ ratio ranging between 16.88 and 54.16 which demonstrates the leaching of ^{234}U except in two samples A6 and A9 (**Figure 4**).

Fernandes et al. [15], Maher et al. [16], Robinson et al. [17], DePaolo [18], and DePaolo et al. [4] have shown that uranium isotopes are leached to the same extent but that the same is not observed for other radionuclides; hence the difference between ^{234}U and ^{238}U leaching percent could represent the ^{234}U percent that resulted from α-recoil as shown in **Table 3** and **Figure 6**. The difference in the resulting values may be related to rock type, as manifested in samples A5 and A6.

Table 3. Transfer of ^{234}U by chemical leaching and physical α-recoil.

Sample		^{234}U (Chemical Transfer)	^{234}U (α-Recoil)
High Silicate	A11	48.21	69.42
High Al Silicate	A7	53.35	40.16
	A8	60.12	29.62
High Carbonate	A1	12.13	16.70
	A2	63.89	-8.75
	A3	39.49	46.20
	A4	28.50	43.55
	A9	55.82	8.18
	A10	56.59	48.27
High Organic Matter (Sulfur)	A5	76.74	5.89
	A6	93.81	2.50

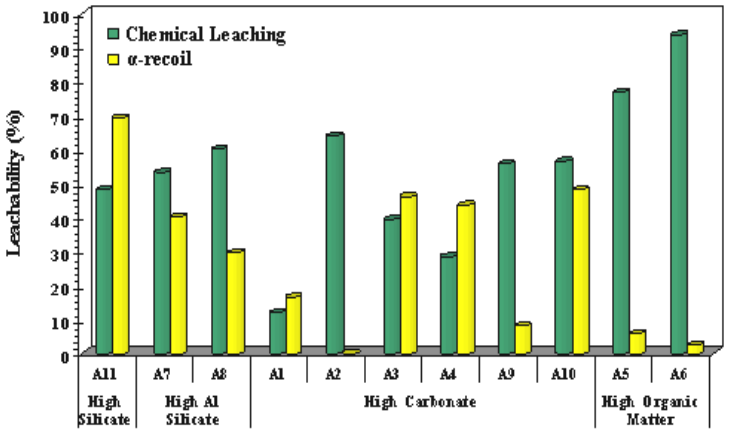

Fig. 6. Chemical and physical transfer of ^{234}U to leachate.

6.5 Residual

The uranium tailings (residual) are essentially the same material as the original ore mineralization with two

differences: a larger surface area and most of the uranium having been extracted by chemical treatment. Most of the radium from the ores appears in the tailings [73]. Uranium mill tailings contain many naturally occurring hazardous substances, both radioactive and non-radioactive, and include approximately 85% of the radioactivity present in the unprocessed uranium ore [74].

The two radionuclides ^{226}Ra and ^{230}Th were found almost totally in the residue (**Table 2**) indicating relatively insoluble mineral phases like alumino silicates and refractory oxides. The lowest values for radionuclides occurring in the residual phase were recorded in marl, representing mainly ^{238}U, ^{235}U, and ^{234}U indicating high leaching efficiency in this rock in contrast to dolostone samples (A1, A2, A3, and A4), in which were recorded the lowest percent of these radionuclides. Noyes [75] mentioned that the tailings from processed uranium ore contain the lowest concentrations of the ^{238}U decay chain: ^{238}U, ^{234}U, ^{230}Th, ^{226}Ra, ^{222}Rn, and the radioactive decay products of ^{222}Rn; they retain about 85% of the total radioactivity of the uranium ore from which they were produced.

Samples A2, A5 (marl), and A10 (shale) displayed $^{234}U/^{238}U$ activity ratios >1, while the other samples had ratios less than unity (**Figure 3**). The $^{234}U/^{238}U$ activity ratios >1 may result from re-adsorption or co-precipitation of ^{234}U by amorphous materials while the $^{234}U/^{238}U$ activity ratios <1 could be related to the presence of refractory minerals rich in uranium in the residual phase. The $^{234}U/^{238}U$ isotope ratio in resistant quartz phases is above unity, attributed to a process of alpha emplacement in these stable, uranium-poor mineral phases [76]. Sheng and Kuroda [77], [78] state that in resistant phases, both $^{234}U/^{238}U$ and $^{230}Th/^{234}U$ activity ratios are above unity, which may be attributed to recoil emplacement processes. It has been demonstrated experimentally that some minerals such as clays or iron/manganese oxide phases are efficient at removing radionuclides from the soluble phase [79]. The organic matter content may also contribute significantly to chemical fractionation between uranium and its long-lived daughters [80].

Samples A5, A6 (marl), A11 (sandstone), and A2, A3 (dolostone) show $^{230}Th/^{238}U$ and $^{230}Th/^{234}U$ >1 (**Figure 3**). The samples A1, A4, and A7 have $^{230}Th/^{238}U$ activity ratios <1. This probably resulted from the leaching of U that was fixed again in the solid phase. Preferential complexation of thorium with dissolved organic matter, which enhances its mobility, and hence leads to depletion in residual compared to uranium, may be the cause of $^{230}Th/^{238}U$ activity ratios <1 [81]. The radioactive disequilibria of $^{230}Th/^{234}U$ are mainly produced by α-decay enhanced dissolution, re-adsorption, and re-precipitation of ^{234}U. Thorium isotopes are significantly associated with colloids [34].

In normal conditions, mobility of Ra, Th, and U has been reported to be in the order U > Ra > Th [6]. Activity concentration of ^{226}Ra in some residual sample is almost five times higher than for ^{238}U (**Table 2**). However, uranium is shown to be much more mobile. Mobility of ^{226}Ra is suppressed by high concentrations of sulfate ions leading to the formation of stable (precipitated) $RaSO_4$, and thus reducing the mobility of radium. Elevated $^{226}Ra/^{238}U$ activity ratios, up to 9, have been reported in organic-rich soil from Cronamuck Valley, Ireland [82].

The $^{238}U/^{235}U$ activity ratios of the residual samples varied between 21.70 and 21.74 (**Figure 4**) which reflects little deviation from the natural ratio (21.7). The residual samples show more diverse results in $^{234}U/^{235}U$ activity ratios, with values ranging between 8.44 and 87.50, reflecting the leaching out/in of uranium (**Figure 4**).

The summation of activities of the measured radionuclides in the pregnant solution and residual in samples (A1, A2, A7, A9, and A10) are higher than the activity of the original, possibly due to the effect of acid solutions during leaching processes which led to cleaning the residual grain surface, thus permitting the gamma activities of the inner grains to be measured [83].

It is worthy of mention that in some investigated samples (A7, A8, A9, and A11), the activity concentration of radium in the residual is higher than in original samples, and this may be related to the greater effect of attenuation in the original sample.

7 CONCLUSIONS

Ten samples of different rock types were collected to study the transfer of different radionuclides from solid material (ore) to the liquid phase (leachate). Activity concentrations and activity ratios of radionuclides in original, leachate, and residual were measured by using a high purity germanium (HPGe) detector. The results show that this transfer was carried out either physically through α-recoil or chemically through dissolution, complexation, chelation, and ion-adsorption. The organic matter content may also contribute significantly to chemical fractionation between uranium and its long-lived daughters. The uranium isotopes are leached to the same extent but that the same is not observed for other radionuclides; hence the difference between ^{234}U and ^{238}U leaching percent could represent the ^{234}U percent that resulted from α-recoil. The difference in the resulting values may be related to rock type. The two radionuclides ^{226}Ra and ^{230}Th were found almost totally in the residue indicating an association with relatively insoluble mineral phases. In some investigated samples, the activity concentration of radium in the residual is higher than in original samples, and this may be related to the greater effect of attenuation in the original sample. The summation of activities of the measured radionuclides in the pregnant solution and residual in some samples are higher than the activity of the original, possibly due to the effect of acid solutions during leaching processes which led to cleaning the residual grain surface, thus permitting the gamma activities of the inner grains to be measured.

ACKNOWLEDGMENTS

We are grateful to the laboratory of HPGe-detector in Nuclear Materials Authority, Egypt for help in the analysis of studied samples.

REFERENCES

[1] M. Vasile, L. Benedik, T. Altzitzoglou, Y. Spasova, U. Watjen, R. Gonza'lez de Orduna, M. Hult, M. Beyermann, and I. Mihalcea, "^{226}Ra and ^{228}Ra determination in mineral waters-Comparison of methods," Applied Radiation and Isotopes, vol. 68, pp. 1236-1239, 2010.

[2] J.L. Aguado, J.P. Bolivar, and R. García-Tenorio, "^{226}Ra and ^{228}Ra determination in environmental samples by alpha-particle spectrometry," Journal of Radioanalytical and Nuclear Chemistry, vol. 278, pp. 191-199, 2008.

[3] I.E. El Aassy, M.M. El Galy, A.A. Nada, M.G. El- Feky, Th.M. Abd El Maksoud, Sh.M. Talaat, and E.M. Ibrahim, "Effect of alteration processes on the distribution of radionuclides in uraniferous sedimentary rocks and their environmental impact, southwestern Sinai, Egypt," Journal of Radioanalytical and Nuclear Chemistry, vol. 289, pp. 173–184, 2011.

[4] D.J. DePaolo, K. Maher, J.N. Christensen, and J. McManus, "Sediment transport time measured with U-series isotopes: Results from ODP North Atlantic drift site 984," Earth and Planetary Science Letters, vol. 248, pp. 394–410, 2006.

[5] A. Dosseto, B. Bourdon, and S.P. Turner, "Uranium-series isotopes in river materials: insights into the timescales of erosion and sediment transport," Earth and Planetary Science Letters, vol. 265, (1–2), pp. 1–17, 2008.

[6] M. Ivanovich, and R.S. Harmon, "Uranium-series disequilibrium: Applications to earth, marine and environmental sciences," Clarendon Press Oxford, 1992.

[7] B. Bourdon, S. Turner, G.M. Henderson, and C.C. Lundstrom, "Introduction to U-series geochemistry," Reveiws in Mineralogy and Geochemistry, vol. 52, pp. 1–21, 2003.

[8] F. Chabaux, J. Riotte, and O. Dequincey, "U–Th–Ra Fractionation during Weathering and River Transport," In: B Bourdon, GM Henderson, CC Lundstrom, SP Turner (Eds.), Uranium-series Geochemistry, Reviews in Mineralogy and Geochemistry, 52. Geochemical Society-Mineralogical Society of America, Washington, pp. 533–576, 2003.

[9] B. Skwarzec, A. Boryio, and D.I. Struminska, "Activity disequilibrium between ^{234}U and ^{238}U isotopes in southern Baltic," Water, Air and Soil Pollution, vol. 159, pp. 165-173, 2004.

[10] X. Jiang, Z. Yu, T.-L. Ku, X. Kang, W. Wei, and H. Chen, "Distribution of uranium isotopes in the main channel of Yellow river (Huanghe), China," Continental Shelf Research, vol. 29, pp. 719-727, 2009.

[11] S. Rezzoug, F. Fernex, H. Michel, G. Barci-Funel, and V. Barci, "Behavior of uranium and thorium isotopes in soils of the Boréon area, Mercantour Massif (S.E. France): Leaching and weathering rate modeling," Journal of Radioanalytical and Nuclear Chemistry, vol. 279, no. 3, pp. 801–809, 2008.

[12] S.Y. Lee, S.J. Kim, and M.H. Baik, "Chemical weathering of granite under acid rainfall environment, Korea," Environ. Geol., vol. 55, pp. 853–862, 2008.

[13] D.M. Bonotto, J.N. Andrews, and D.P.F. Darbyshire, "A laboratory study of the transfer of ^{234}U and ^{238}U during water-rock interaction in the Carnmenellis granite (Cornwall, England) and implication for the interpretation of field data," Applied Radiation and Isotopes, vol. 54, pp. 977-994, 2001.

[14] M.B. Andersen, Y. Erel, and B. Bourdon, "Experimental evidence for ^{234}U-^{238}U fractionation during granite weathering with implication for ^{234}U/^{238}U in natural waters," Geochim. Cosmochim Acta, vol. 73, pp. 4124-4141, 2009.

[15] H.M. Fernandes, M.R. Franklin, and L.H. Veiga, "Acid rock drainage and radiological environmental impacts. A study case of the Uranium mining and milling facilities at Poc,os de Caldas," Waste Management, vol. 18, pp. 169-181, 1998.

[16] K. Maher, D.J. DePaolo, and J.C.F. Lin, "Rates of silicate dissolution in deep-sea sediment: In situ measurement using U-234/U-238 of pore fluids," Geochim Cosmochim Acta, vol. 68, pp. 4629–4648, 2004.

[17] L.F. Robinson, G.M. Henderson, L. Hall, and I. Matthews, "Climatic control of riverine and seawater uranium-isotope ratios," Science, vol. 305, pp. 851–854, 2004.

[18] D.J. DePaolo, "Isotopic effects in fracture-dominated reactive fluid–rock systems," Geochimica et Cosmochim Acta, vol. 70, pp. 1077–1096, 2006.

[19] IAEA "Preparation and Certification of IAEA Gamma Spectrometry Reference Materials, RGU-1, RGTh-1 and RGK-1," International Atomic Energy Agency. Report-IAEA/RL/148, 1987.

[20] R.M. Anjos, R. Veiga, T. Soares, A.M.A. Santos, J.G. Aguiar, M.H.B.O. Frascá, J.A.P. Brage, D. Uzêda, L. Mangia, A. Facure, B. Mosquera, C. Carvalho, and P.R.S. Gomes, "Natural Radionuclide Distribution in Brazilian Commercial Granites," Radiation Measurements, vol. 39, pp. 245–253, 2005.

[21] R.A. Sutherland, and E. de Jong, "Statistical Analysis of Gamma-Emitting Radionuclide Concentrations for Three Fields in Southern Saskatchewan, Canada," Health Physics, vol. 58, no. 4 (April), pp. 417–428, 1990.

[22] Y. Yokoyama, C. Falguères, F. Sémah, T. Jacob, and R. Grün, "Gamma-Ray Spectrometric Dating of Late Homo Erectus Skulls from Ngandong and Sambungmacan, Central Java, Indonesia," Journal of Human Evolution, vol. 55, pp. 274–277, 2008.

[23] H. Yücel, A.N. Solmaz, E. Köse, and D. Bor, "Methods for Spectral Interference Corrections for Direct Measurements of ^{234}U and ^{230}Th in Materials by Gamma-Ray Spectrometry," Radiation Protection Dosimetry, vol. 138, no. 3, pp. 264–277. doi:10.1093/rpd/ncp239, 2010.

[24] H. Ramebäck, A. Vesterlund, A. Tovedal, U. Nygren, L. Wallberg, E. Holm, C. Ekberg, and G. Skarnemark, "The Jackknife as an Approach for Uncertainty Assessment in Gamma Spectrometric Measurements of Uranium Isotope Ratios," Nuclear Instruments and Methods in Physics Research B: Beam Interactions with Materials and Atoms, vol. 268, no. 16, pp. 2535–2538, 2010.

[25] J.J. Simpson, and R. Grün, "Non-Destructive Gamma Spectrometric U-Series Dating," Quatern Geochrono, vol. 17, pp. 1009–1022, 1998.

[26] H. Yücel, M.A. Cetiner, and H. Demirel, "Use of the 1001 keV Peak of ^{234m}Pa Daughter of ^{238}U in Measurement of Uranium Concentration by HPGe Gamma-Ray Spectrometry," Nuclear Instruments and Methods in Physics Research, Section A, vol. 413, pp. 74–82, 1998.

[27] R. Pöllänen, T.K. Ikäheimonen, S. Klemola, V.P. Vartti, K. Vesterbacka, S. Ristonmaa, T. Honkamaa, P. Sipilä, I. Jokelainen, A. Kosunen, R. Zilliacus, M. Kettunen, and M. Hokkanen, "Characterization of Projectiles Composed of Depleted Uranium," Journal of Environmental Radioactivity, vol. 64, pp. 133–142, 2003.

[28] L. Shapiro, and W.W. Brannock, "Rapid Analysis of Silicates, Carbonates and phosphate Rocks, U.S," Geol. Surv. Bull., 114 A, 1962.

[29] S.M.B. Siddeeg, "Geochemistry of natural radionuclides in uranium-enriched river catchments," Ph.D. Thesis, Faculty of Engineering and Physical Science, University of Manchester, 189p, 2013.

[30] S.R. Taylor, and S.M. McLennan, "The Continental Crust; Its composition and evolution; an examination of the geochemical record preserved in sedimentary rocks," Blackwell, Oxford, 312, 1985.

[31] Y. Dawood, "Radiogenic Isotope Fractionation as an Indication for Uranium Mobility in the Granites of El Shallal Area, West Central Sinai, Egypt," JKAU; Earth Sci, vol. 20, pp. 215-238, 2009.
[32] M. Maozhong, P. Xinjian, W. Jinping, and J.K. Osmond, "Uranium-series disequilibria as a means to study recent migration of uranium in a sandstone-hosted uranium deposit, NW China," Applied Radiation and Isotopes, vol. 63, pp. 115–125, 2005.
[33] M.M. Sarin, K. Krishnaswami, B.L.K. Somayajulu, and W.S. Moore, "Chemistry of uranium, thorium, and radium isotopes in the Ganga-Brahmaputra river system: Weathering processes and fluxes to the Bay of the Bengal," Geochim Cosmochim Acta, vol. 54, pp. 1387–1396, 1990.
[34] S.A. Short, "Chemical transport of uranium and thorium in the Alligator river uranium province, Northern Territory, Australia," University of Wollongong Thesis collections, 1988.
[35] R.T. Lowson, S. Short, B.G. Davey, and D.J. Gray, "$^{234}U/^{238}U$ and $^{230}Th/^{234}U$ activity ratios in mineral phases of a lateritic weathered zone," Geochim Cosmochim Acta, vol. 50, pp. 1697-1702, 1986.
[36] D. Mathieu, M. Bernat, and D. Nahon, "Short-lived U and Th isotope distribution in a tropical laterite derived from granite (Pitinga river basin, Amazonia, Brazil): Application to assessment of weathering rate," Earth and Planetary Science Letters, vol. 136, pp. 703-714, 1995.
[37] N. Yanase, T.E. Payne, and K. Sekine, "Groundwater geochemistry in the Koongarra ore deposit, Australia (1): Implication for uranium migration," Geochem J, vol. 29, pp. 1-29, 1995a.
[38] N. Yanase, T.E. Payne, and K. Sekine, "Groundwater geochemistry in the Koongarra ore deposit, Australia (II): Activity ratios and migration mechanisms of uranium series radionuclides," Geochem. J., vol. 29, pp. 31-54, 1995b.
[39] C. Lin, T. Chu, and Y. Huang, "Variations of U/Th-series nuclides with associated chemical factors in the hot spring area of northern Taiwan," Journal of Radioanalytical and Nuclear Chemistry, vol. 258, no. 2, pp. 281-286, 2003.
[40] N.A. Saad, B.I. Zidan, and I.K. Khalil, "Geochemistry and origin of the manganese deposits in the Umm Bogma region, west central Sinai, Egypt," Journal of African Earth Sciences, vol. 19(1–2), pp. 109-116, 1994.
[41] M.R. Khattab, "The $^{234}U/^{238}U$ ratios and Water Chemistry for Underground Water Characterizations in Different localities (Sinai and Western Desert, Egypt)," Ph.D. Thesis, Menoufiya University, 141p, 2014.
[42] D. Langmuir, "Uranium solution–mineral equilibria at low temperatures with applications to sedimentary ore deposits," Geochim Cosmochim Acta, vol. 42, pp. 547–569, 1978.
[43] Y. Fujii, M. Nomura, H. Onitsuka, and K. Takeda, "Anomalous Isotope Fractionation in Uranium Enrichment Process," Journal of Nuclear Science and Technology, vol. 26, pp. 1061–1064, 1989.
[44] J. Bigeleisen, "Nuclear size and shape effects in chemical reactions. Isotope chemistry of the heavy elements," J. Am. Chem. Soc., pp. 3676–3680, 1996.
[45] E.A. Schauble, "Role of nuclear volume in driving equilibrium stable isotope fractionation of mercury, thallium, and other very heavy elements," Geochim Cosmochim Acta, vol. 71, pp. 2170–2189, 2007.
[46] E.A. Schauble, "Equilibrium Uranium Isotope Fractionation by Nuclear Volume and Mass-dependent Processes," Eos, vol. 87, December Supplement, abs. V21B-0570, 2006.
[47] G.A. Brennecka, L.E. Borg, I.D. Hutcheon, M.A. Sharp, and A.D. Anbar, "Natural Variations in Uranium Isotope Ratios of Uranium Ore Concentrates: Understanding the $^{238}U/^{235}U$ Fractionation Mechanism," Earth and Planetary Science Letters, vol. 291, pp. 228–233, 2010.
[47] S. Weyer, A.D. Anbar, A. Gerdes, G.W. Gordon, T.J. Algeo, and E.A. Boyle, "Natural fractionation of $^{238}U/^{235}U$," Geochim Cosmochim Acta, vol. 72, pp. 345–359, 2008.
[48] C. Montoya-Pino, S. Weyer, A.D. Anbar, J. Pross, W. Oschmann, B. Schootbrugge, H.W. Arz, "Global enhancement of ocean anoxia during Oceanic Anoxic Event 2: A quantitative approach using U isotopes," Geology, vol. 38, pp. 315–318, 2010.
[49] Y.A. Uvarovaa, T.K. Kyser, M.L. Geagea, and D. Chipley, "Variations in the uranium isotopic compositions of uranium ores from different types of uranium deposits," Geochimica et Cosmochimica Acta, vol. 146, pp. 1–17, 2014.
[50] Y. Eyal, "Preferential leaching and the age of radiation damage from alpha decay in minerals," Geochim Cosmochim Acta, vol. 49, pp. 1155-l164, 1985.
[51] V. Benes, A.V. Boitsov, M. Fuzlullin, J. Hunter, W. Mays, J. Novak, and D.H. Underhill, "Manual of Acid in situ Leach Uranium Mining Technology," International Atomic Energy Agency Vienna, 2001.
[52] P. Longmire', "Trace metal and radionuclide adsorption during diagenesis of acid leach uranium tailings, Colorado Plateau," Abstr. Programs Geol. Soc. Am., vol. 15, no. 5, 313, 1983.
[53] P. Longmire', W. Turney, C. Mason, D. Dander, and D. York, "Predictive geochemical modeling of uranium and other contaminants in laboratory columns in relatively oxidizing carbonate-rich solutions," Technol. Programs Radioact. Waste Mange. Environ. Restor., vol. 3, pp. 2081-2085, 1994.
[54] T.E. Payne, and P.L. Airey, "Radionuclide migration at the Koongarra uranium deposit, Northern Australia – Lessons from the Alligator Rivers analogue project," Physics and Chemistry of the Earth, vol. 31, pp. 572–586, 2006.
[55] T.E. Payne, R. Edis, L. Herczeg, K. Sekine, T. Seo, T.D. Waite, and N. Yanase, "Groundwater chemistry Alligator Riven Analogue Project," Final Report 7, Australian Nuclear Science and Technology Organisation, 1994.
[56] N. Yanase, T. Nightingale, T. Payne, and P. Duerden, "Uranium distribution in mineral phases of rock by sequential extraction procedure," Radioch inn Acta, 52/53, pp. 387-393, 1991.
[57] S.K. Singh, T.K. Dalai, and S. Krishnaswami, "^{238}U series isotopes and ^{232}Th in carbonates and black shales from the Lesser Himalaya: implications to dissolved uranium abundances in Ganga-Indus source waters," J. Environ. Rad., vol. 67, pp. 69–90, 2003.
[58] E.M. Ibrahim, "Behavior of Radionuclides in U-Series during Processing of Uranium Bearing Rock Materials," Ph.D. Thesis, Faculty of Women for Art, Science and Education, Physics Department, Ain Shams University, 207p, 2012.
[59] J.P. Adloff, and K. Röessler, "Recoil and transmutation effects in the migration behaviour of actinides," Radiochimica Acta, vol. 52, no. 1, pp. 269–274, 1991.
[60] J. Suksi, K. Rasilainen, J. Casanova, T. Ruskeeniemi, R. Blomqvist, and J.A.T. Smellie, "U-series disequilibria in a groundwater flow route as an indicator of uranium migration processes," Journal of Contaminant Hydrology, vol. 47, no. 2, pp. 187–196, 2001.
[61] B. Satybaldiyev, J. Lehto, J. Suksi, H. Tuovinen, B. Uralbekov, and M. Burkitbayev, "Understanding sulphuric acid leaching of uranium from ore by means of $^{234}U/^{238}U$ activity ratio as an indicator," Hydrometallurgy, vol. 155, pp. 125–131, 2015.
[62] J.K. Osmond, and M. Ivanovich, "Uranium-series mobilization and surface hydrology," In: Uranium-Series Disequilibrium: Application to Earth, Marine, and Environmental Sciences Oxford Sciences Publications Oxford, pp. 259–289, 1992.
[63] M. Min, H. Xu, J. Chen, and M. Fayek, "Evidence of uranium bio-mineralization in sandstone-hosted roll-front uranium deposits, northwestern China," Ore Geology Reviews, vol. 26, pp. 198-206, 2005.
[64] K. Kigoshi, "Uranium dating of igneous rocks," Science, vol. 156, pp. 932–934, 1967.
[65] R. Tanaka, T. Yokoyama, H. Kitagawa, D.B. Tesfaye, and E. Nakamura, "Evaluation of the applicability of acid leaching for the ^{238}U–^{230}Th internal isochron method," Chemical Geology, vol. 396, pp. 255–264, 2015.

[66] D. Langmuir, and D. Melchior, "The geochemistry of Ca, Sr, Ba and Ra sulfates in some deep brines from the Palo Duro Basin, Texas," Geochim Cosmochim Acta, vol. 49, pp. 2423-2432, 1985.
[67] D. Langmuir, and A.C. Riese, "The thermodynamic properties of radium," Geochim Cosmochim Acta, vol. 49, pp. 1593-1601, 1985.
[68] B.L. Dickson, and A.A. Swelling, "Movements of uranium and daughter isotopes in the Koongarra uranium deposit," Uranium in the Pine Creek Geo- syncfiue (Ferguson, J., Ooteby, A.B., eds.), pp. 499-507, IAEA Vienna, 1980.
[69] P. Benes, "Radium in (continental) surface water," The Environmental Behaviour of Radium (IAEA ed.), 373Ml8, Vienna, 1990.
[70] T. Murakami, H. Lsobe, and R. Edis, "Effects of chlorite alteration on uranium redistribution in Koongarra, Australia," Mat. Res. Soc. Symp. Proc., vol. 212, pp. 741-748, 1990.
[71] C.H. Stirling, M.B. Andersen, E.-K. Potter, and A.N. Halliday, "Low-temperature isotopic fractionation of uranium," Earth and Planetary Science Letters, vol. 264, pp. 208–225, 2007.
[72] M.J. Murphy, C.H. Stirling, A. Kaltenbach, S.P. Turner, and B.F. Schaefer, "Fractionation of $^{238}U/^{235}U$ by reduction during low temperature mineralisation processes," Earth and Planetary Science Letters, vol. 388, pp. 306–317, 2014.
[73] V.I. Lakshmanan, and A.W. Ashbrook, "Radium balance studies at the Beaverlodge mill of Eldorado," Nuclear Ltd., OECD/NEA Seminar, Albuquerque NM p.51, 1978.
[74] D.R. Metzler, "Uranium Mining: Environmental Impact," Encyclopedia of Energy, vol. 6, pp. 299-315, 2004.
[75] R. Noyes, "Nuclear Waste Cleanup Technology and Opportunities," William Andrew Inc. ISBN: 978-0-8155-1381-0, 471 p, 1995.
[76] B.J. Szabo, "Extreme fractionation of $^{234}U/^{238}U$ and $^{230}Th/^{234}U$ in spring waters, sediments and fossils at the Pomme de Terre Valley, southwestern Missouri," Geochim Cosmochim Acta, vol. 46, pp. 1675-1679, 1982.
[77] Z.Z. Sheng, and P.K. Kuroda, "Isotopic fractionation of uranium: extremely high enrichments of ^{234}U in the acid-residues of a Colorado carnotite," Radiochim Acta, vol. 39, pp. 131-138, 1986a.
[78] Z.Z. Sheng, and P.K. Kuroda, "Further studies on the separation of acid residues with extremely high $^{234}U/^{238}U$ ratios from a Colorado carnotite," Radiochim Acta, vol. 40, pp. 95-102, 1986b.
[79] M.C. Duff, J.U. Coughlin, and D.B. Hunter, "Uranium co-precipitation with iron oxide minerals," Geochimica et Cosmochim Acta, vol. 66, pp. 3533-3547, 2002.
[80] A. Dosseto, B. Bourdon, J. Gaillardet, L. Maurice-Bourgoin, and C.J. Allegre, "Weathering and transport of sediments in the Bolivian Andes: Time constraints from uranium-series isotopes," Earth and Planetary Science Letters, vol. 248, pp. 759-771, 2006.
[81] A.J. Plater, M. Ivanovich, and R.E. Dugdale, "Uranium series disequilibrium in river sediments and waters: the significance of anomalous activity ratios," Applied Geochemistry, vol. **7**, pp. 101-110, 1992.
[82] M. Dowdall, and J. O'Dea, "$^{226}Ra/^{238}U$ disequilibrium in an upland organic soil exhibiting elevated natural radioactivity," Journal of Environmental Radioactivity, vol. 59, pp. 91-104, 2002.
[83] A. Nada, and E.M. Ibrahim, "Relation between radionuclides activities before and after leaching processes of different rock types," Journal of Applied Sciences Research, vol. 9, no. 6, pp. 3536-3542, 2013.